# SCIENTIFIC EXPERIMENTS FOR TEMPORAL AND SPATIAL RELATIONSHIPS BETWEEN HILLSLOPE AND KNICK POINT RETREAT

**Dr. N.L. Dongre.**


**Photographs of Kegon Falls prior to and following the 1986 collapse. (A) Kegon Falls in 1965; (B) Kegon Falls in 2011 (photograph taken by the Yuichis Hayakawa-2013 ). Approximate extent of the 1986 rockfall is indicated by the white dashed line.**

**Abstract**

*Hillslope stability depends heavily on local conditions, such as lithology and rock strength, degree of saturation, and critical slope angle. Common triggers for slope failure include intense storms, earthquakes, and removal of material from the toe of the hillslope. In this article, it is observed on the latter, in a model in which streams incise the toe and destabilize the hillslope. It is investigated interactions between migrating knickpoints and hillslope failures in a small-scale, steadily eroding experimental landscape that experiences steady rainfall and base-level fall conditions. It is observed and checked knickpoint assistance and hillslope failure activity with time lapse photography over a time period in which numerous knickpoints migrated through the drainage basin. It is then experimented temporal and spatial co-relations between hillslope failures and knickpoints and compared these results to Monte Carlo system simulations of hillslope failure distributions. When concentrating along a single channel, it is found that, statistically (significant at the 98% confidence level), a large number of failures happen downstream from a migrating knickpoint. These results highlight both the organized and random nature of hillslope and knickpoint interactions.*

## Introduction

Landslides play a vital role in denudational processes in eroding drainage basins. There is significant motivation to understand the controls of landslide initiation, as well as the timing, location, and size of landslides. In this article, it is studied stream and hillslope interactions in a controlled experimental drainage basin. It is tested the hypothesis that stream incision driven by migrating knick-points can apply a spatial and temporal pattern on landslide distributions.

The controls on landsliding involve few important variables, including lithologic structure, soil conservation and structure, pore fluid pressure, topographic setting, and vegetation. A Mohr-

Coulomb relation between stress and failure forms the platform for estimating the critical stress at which a hillslope will fail. There are many ways for the motion threshold to be exceeded. Common results include severe rain storms, where increased pore fluid pressure facilitates failure, earthquakes, where ground shaking induces failure, and removal of material and support from the toe of the hillslope. This last mechanism in the study is investigated. Vegetation covers control on substrate resistance, and this adds further complexity to the susceptibility of hillslope failure (Sidle, 1992; Duan, 1996; Montgomery et al., 2000; Gabet and Dunne, 2002).

Spatial and temporal assessment provides an estimate of the contribution of landsliding to the erosional budget for landscapes, and offer related elements for forcasting landslide events in any region. In greater way, physics-based modelling has co-related topographic and weather information with stability system, and this approach offers predictions for the location and timing of landsliding. Landslide size-frequency studies have also employed physical experiments (Densmore et al., 1997) in which a simulated granular hillslope composed of beans responded to base-level fall.

The reason behind local conditions that control hillslope stability, one might expect that landslide happenings are stochastic in time and space. Some spatial patterning results from the origination of shallow landslides in hollows in low-order drainages (Campbell, 1975; Montgomery and Dietrich, 1994; Benda and Dunne, 1997). In this subject, the spatial pattern is governed by drainage basin structure. Temporal patterns of landslides are largely related to triggering by storm or earthquake events. However, time series of shallow landslides generated from experimental (Densmore et al., 1997) and physics-based models (Benda and Dunne, 1997) are highly stochastic, emphasizing the sensitivity to local conditions.

Now it is proceeded to an additional means of destabilizing hill-slopes in natural settings: removal of material from the toe of the hillslope by streams. This mechanism has received less attention, largely due to the longer time scales involved in stream incision. While bedrock incision by streams involves a variety of mechanisms it is focused on two styles of stream incision in this study: a steady profile lowering due to uniform erosion of the bed, and knickpoint migration.

Knickpoints can play a important role in river incision and valley development (Ahnert, 1998). Knickpoints are step changes in bed surface elevation where intense, localized erosion takes place. Formation of knickpoints and their upstream migration have been connected to concentration of overland flow. They are an important erosional process in bedrock channels (Miller, 1991), and landscape evolution. The mechanism of upstream knickpoint migration has been the object of several experimental, theoretical, and field studies (Brush and Wolman, 1960; Holland and Pickup, 1976; Gardner, 1983; Bryan and Rockwell, 1998; Bennett et al., 2000; Parker and Izumi, 2000; Alonso et al., 2002; Crosby and Whipple, 2002), where the effects of varying bed material, water table height, slope, and flow discharge on migration rate have been explored.

Though innumarable studies of hillslope stability, river incision, and knickpoint behavior have been conducted, these studies have not observed into a systematic co-relations between knickpoint propagation and hillslope failure activity. There are good reasons for this omission. Knickpoints in bedrock channels require a significant amount of time to propagate up through a drainage basin, and so field studies of stream incision and hillslope response are limited by the length of time required to observe this kind of behavior in natural landscapes. Hillslope adjustment to a lowering river bed via landsliding has been documented as a significant response by Burbank et al. (1996) in the north-western Himalaya, but the connection between stream incision and knick-point propagation is not known for this case.

It is pursued that the resul of stream incision on hillslope stability through postulating that hillslope failures should exhibit spatial and temporal patterns controlled by knickpoint propagation. like, if a stream is actively downcutting at the toe of the hillslope, and stream incision is due to the migration of a knickpoint, then hillslope failures will follow in the wake of the knickpoint. As per to this assumption, knickpoint location and migration should have an influence on the spatial and temporal patterns of landslides. A small experimental drainage basin provides a convenient setting to test the strength of coupling between stream incision and hillslope failures. The research by Hasbargen and Paola 2000, 2003; Lague et al., 2003 has demonstrated the utility of monitoring experimental eroding landscapes under steady uplift and rainfall conditions. These experiments have documented hillslope failures and knickpoints as common erosional processes within laboratory drainage basins (Hasbargen, 2003). Consequently, basic interactions between stream incision and

failures can be studied in a controlled environment, and they provide a suitable setting to test the idea that knick-points impose a spatial and temporal pattern of failures in their wake. In brief, hillslope failures come in a variety of sizes and styles of movement. It is recognized the diverse character of mass movements on hillslopes in natural settings, it is used the terms "hillslope failure" and "landslide" interchangeably throughout this paper. Because weathering and soil development are unavailable in the experimental landscape, shallow landslides of soil are absent in the experiment. Landslides in the erosional facility are analogous to deep-seated bedrock landslides.

**Account of the Experimental Apparatus**

Hasbargen and Paola, 2000; Hasbargen, 2003 has observed the laboratory experiments and following them a small-scale physical experimental apparatus was set up at Jaypee Laboratory of Jaypee Nagar, Rewa The apparatus contended of a nearly circular steel tank ~1 m in diameter and 1 m deep with a single outlet dammed by a motor-controlled gate (Fig. 1). The outlet was 1 cm wide. A motor was attached to the sliding gate via a cable. The motor was run continuously during the experiment, dropping the outlet at a slow, constant rate. The effect of dropping base level is equivalent to uniform block uplift of the basin relative to base level. Numerous measurements were taken of the outlet height during the experiment to verify steady base-level fall. A set of 8 greenhouse misters placed 70 cm above the upper level of the tank sprinkled rain (droplet size <200 μm)Over basin, generating run off. A pressure regulator maintained a constant pressure to the mist apparatus.

The function of this experimental system under different conditions has been observed. For the present study, it is carried out detailed measurements of landslide distribution and knickpoint migration in one experiment. The experimental conditions were: rainfall rate = 10.83 μm/s, base-level fall rate = 3.1 lμm/s. Before beginning the experiment, it is calibrated the rainfall spatial distribution by collecting rainfall in pans at the top of the basin. The spatial coefficient of variation was <15% over a measurement interval of 12 min ($n$ = 27). At the beginning of the experiment, the basin was filled with erodible material consisting of a well-sorted silica silt ($D_{50}$ = 45 μm) mixed with kaolinite (1% by weight). These were mixed with water to the consistency of medium cement in a cement mixer, poured into the basin, and allowed to settle overnight.

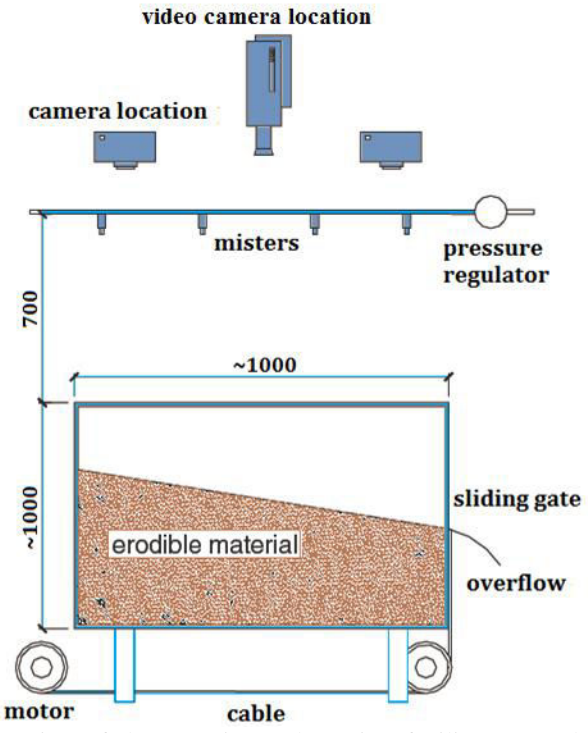


Figure 1. Schematic cross section of the experimental erosion facility. A steel cable drops the outlet; it is wrapped on a pulley and driven by an electric motor mounted on the floor. Dimensions are in millimeters

After initial calibration of rainfall and base-level fall rate, it was initiated that the experiment by turning on the motor-controlled outlet and rainfall. The run lasted for 64 h, at which time the sliding gate outlet reached the bottom of the basin. Initially, the surface was flat, and runoff patterns were essentially random (Fig. 2). After complete dissection of the initial surface, a 3-5 order drainage network had developed (Fig. 3). The dissection of the initial flat surface required ~16 h. Digital stereo-images (1280 ×960 pixel resolution) of the basin were collected at 8-10 min intervals. Time-lapse video recorded snapshots every 100 s. Sediment flux at the basin outlet was measured by weighing sediment and water in a handheld graduated cylinder, and recording the time required to fill it. It was episodically applied that a thin veil of colored sand over the surface as a tool for the identification of topographic features, such as terraces (Fig. 4) and hillslope failures (Fig. 5). The erosion of the colored sand provided an indication of both the length of time required to erode the surface, and a visual record of spatially variable erosion.

350 photographs were collected, of which 100 were selected for mapping the position of knickpoints and the location and size of hillslope failures. These 100 photographs covered the last part of the experiment, an interval of 14 h, during which time the landscape eroded at a flux steady-state condition, an amount of time sufficient for the landscape to erode through 15 cm of the substrate, or ~1 unit of local relief (12 cm).

## EXPERIMENTAL OUTPUT

### Qualitative Observations of Drainage Basin Dynamics

in spite of temporally steady external forcing and flux steady-state conditions, the drainage network exhibited interesting non-steady dynamic behavior, as observed in the experiments. It was noted short-term processes, such as hillslope failures and runoff-based erosion; intermediate time-scale processes, such as knickpoint development and

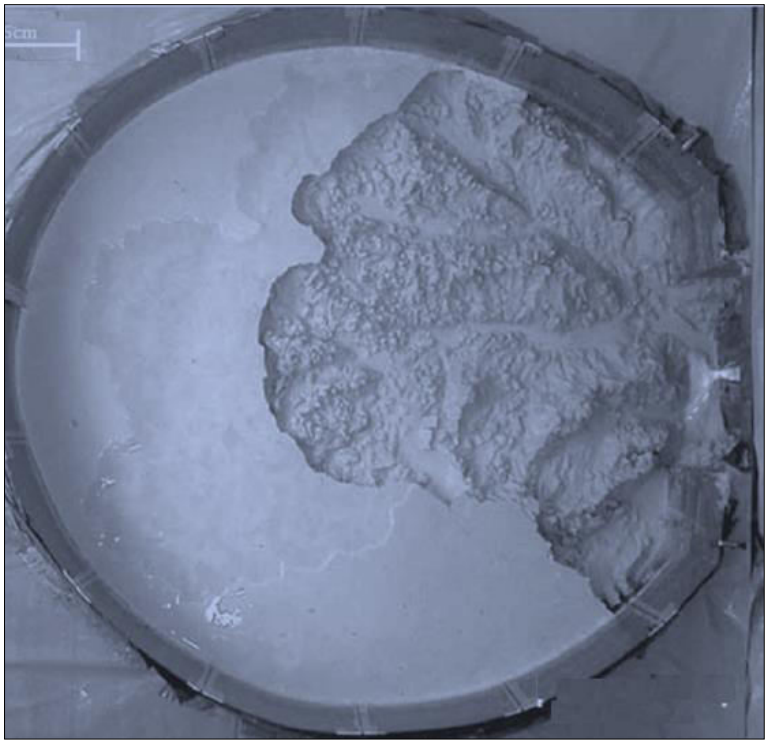

Figure 2. Vertical view of the experimental basin at the beginning of the run during dissection of the initial flat surface.

Figure 3. Vertical view of the dendritic pattern of the drainage network. The photo Was taken long after complete dissection of the initial surface (note rind near the top the basin walls) at run time 62:13 h. Outlet is at left center. Basin length (left to right) is 98 cm; basin width (top to bottom) is 86 cm.


Figure 4. Image of the experimental basin showing wide valley of trunk stream, diagnostic of temporary sediment storage; knick point incising into trunk stream; and island and terrace-like structures in the tributary channel in the lower portion of image.

migration, and temporary sediment storage in trunk valleys; and long-term behavior marked by lateral ridge crest movements. Runoff-based erosion was the dominant mechanism for removing material from the basin; it was also the most difficult to detect visually, because flows were rarely more than a few mm deep. It was observed knick points that typically initiated in the lower reaches of the basin and propagated upstream, apparently triggering hillslope failures. Rainfall was necessarily stopped before collecting photographs. Advantage was taken of these occasions to determine how long surface runoff persisted after cessation of rainfall. Flow at the outlet approached nil within a few seconds, implying rapid draining of groundwater from hillslopes and/or very low trans-missivity of groundwater in the substrate. Overall, it could not be detected obvious effects on landscape development from rainfall cessation and recommencement. Hillslope failures were easier to detect than surface runoff erosion and appeared as abrupt shifts in ridge crest location and as concave hillslopes with a slump at the hillslope toe (Fig. 5). Episodic cycling between temporary sediment storage in trunk streams and excavation of stored sediment by knickpoints marked the evolution of the landscape throughout the entire Experiment. During times of temporary sediment storage, trunk streams exhibited wide, smooth valley floors with no clearly defined channel. Sediment storage occupied up to 15% of the basin surface area at any one time. Depositional episodes ended when a knickpoint initiated and migrated upstream. Streams deepened and narrowed and rapidly flushed out stored sediment. Similar types of behavior have been noted for experimental channels following an abrupt base-level drop. After the passage of the knickpoint, sediment storage began again, and the sequence was repeated. In some cases, a smooth valley floor developed more than one channel as a knickpoint propagated upstream. Some channels developed marked sinuosity, though most reaches were straight. Braided channels were not observed, though around knickpoints some islands developed. The time scale for a cut and fill cycle ranged from 1 to 1.55 h, equivalent to 1.1-1.7 cm of base-level fall. When this fall distance is scaled to the typical knickpoint height, the cut/fill cycle time is equivalent to the time needed for ~2 knickpoint heights of erosion.

**Measurements of Hillslope Failure, Knickpoint, and Temporary Sediment Storage Area**

The following measures are offered to give an approximate scale of the experimental landscape, and to facilitate comparison to natural drainage basins. A few digital elevation models (DEMs) were extracted from stereo photographic snapshots of the basin during the course of the experiment to provide basic topographic information (see Fig. 6).

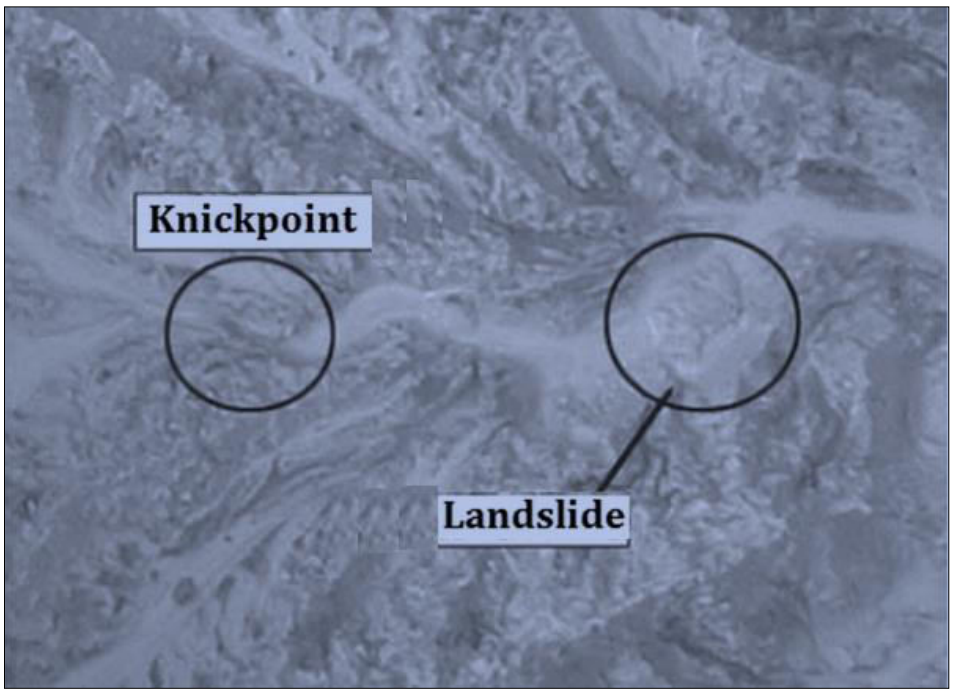


Figure 5. Close-up view of a hill slope failure in the trunk stream after the passage of a knick point. Approximate width of image is ~25 cm.

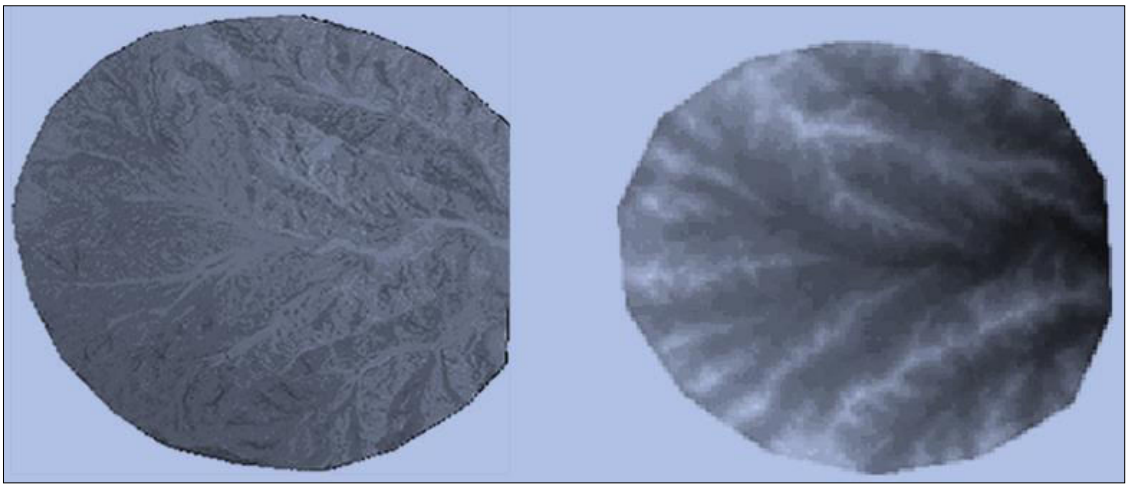

Figure 6. Grayscale digital elevation map (DEM) with pits removed (left), and vertical photograph (right, July 18, photo 17, run time 54:16 h). Long dimension of each image is 90 cm, and width is 86 cm. Grid spacing for DEM is 0.5 cm. Total relief is 22 cm; local relief is 11 cm.

Maximum relief was 26 cm in the experiments, with local ridge-to-valley relief of 10-12 cm. Maximum relief divided by basin length (100 cm) yielded a regional slope value of 0.26. Mean steepest descent slope computed at 6 mm grid spacing was 0.90. Hillslope lengths (distance from divide to channel) ranged from 1 to 10 cm. Low-order channel widths were 0.1-0.2 cm, and trunk valley widths during times of sediment storage ranged up to 5 cm. Upon dissection by a knickpoint, channel widths of trunk streams decreased to ~1 cm. Experimental hillslope failures commonly extended from ridge crest to valley floor, and ranged in size from 1 to 50 $cm^2$. As noted earlier, shallow landslides associated with soil development were absent in the experimental basin. The hillslope failures in the experiment are more appropriately thought of as deep-seated landslides. Topographic profiles of a few failures and a lower-order channel were presented in Figures 7 and 8. Relief of most knickpoints was ~0.5 cm, or 5% of the local ridge-to-valley relief. However, some

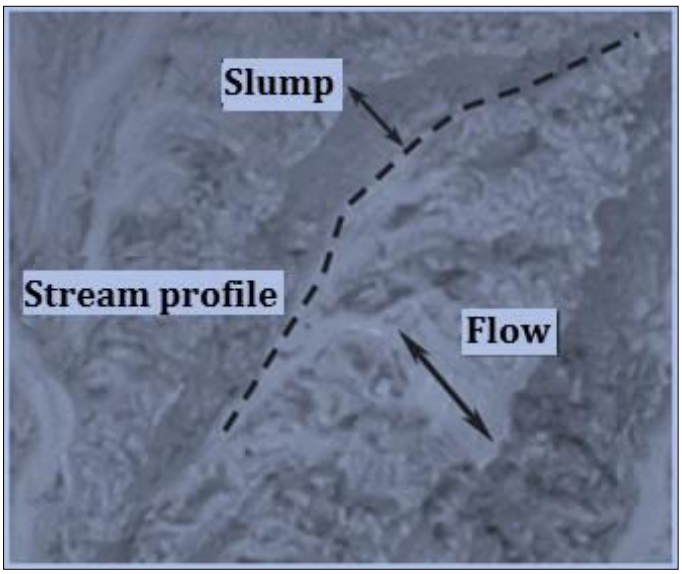


Figure 7. Vertical photograph of two mass movements on hillslopes, showing the location of slump, flow, and stream profile for which topographic profiles were extracted from a digital elevation model (run time, h:min = 54:16).

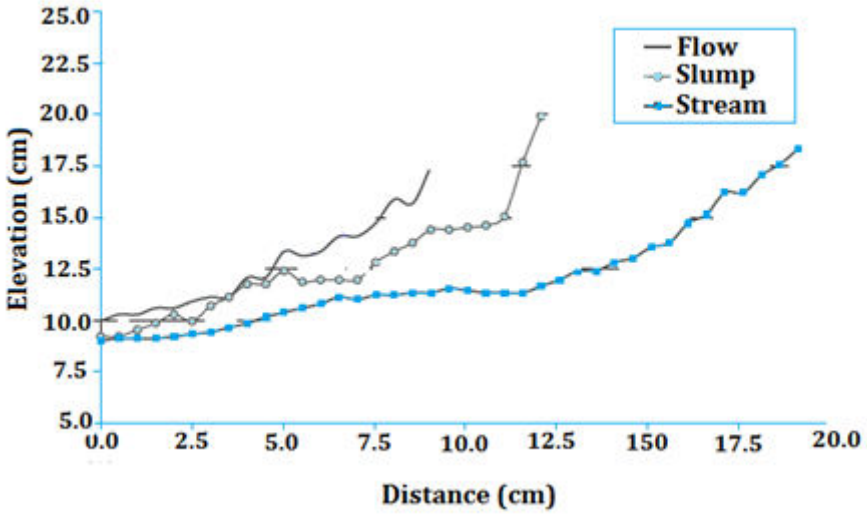


Figure 8. Example of hillslope and channel profiles in the experimental landscape depicted on Figure 7. The feature designated flow appears to be a mass flow, and the feature designated slump exhibits signs of a scarp and irregular deposit at the toe of the hillslope. A stream profile for a second-order channel is plotted to provide a lower limit for relief.

knickpoints exhibited heights of 1-2 cm (10%-20% of local relief). Flat surfaces resembling terraces were noted during this experiment (Fig. 4). They were small, with surface area of 10-20 $cm^2$. They typically persisted for relatively long times (about 1 h on average, which was the time required to erode through ~1 cm, or 10% of local relief in the basin). Interestingly, all of these features, when scaled to appropriate vertical and horizontal length scales, such as the hillslope length and local relief, are of the same order as natural mountainous landscapes.

In order to analyze the spatial distribution of hillslope failures, it was examined that a total of 96 images taken during the last 13 h of the experiment. During this period, base level fell 14 cm, a distance roughly 50% of the total relief of basin. 505 hillslope failures were mapped, and was noticed that the landslide trace remained visible for about two minutes after collapse. Since the time step between photographs was about seven minutes, it is likely that not all of the hillslope failures that occurred between photographic snapshots were mapped.

The surface area and centroid location of each landslide were manually determined on scaled photographs using the image processing software Scion Image. Table 1 reports statistics computed on the mapped failures. The hillslope failures detected had a mean area of 11.1 $cm^2$ and a standard deviation of 9.7 $cm^2$. The smallest recorded failure had an area of 1.4 $cm^2$; the largest had an area of 62 $cm^2$. Smaller events were more numerous than large ones. The size-frequency distribution of landslides can be approximated by a power law with decreasing numbers of larger events (Fig. 9). This result is comparable to those of studies of hillslope failures in natural settings (e.g., Hovius, et al. 1997; Stark and Hovius, 2001; Guzzetti et al., 2002; Brardinoni and Church, 2004), although ideally a much larger number of events over a broader size range would better define such a relation.

**TABLE 1. MAIN CHARACTERISTICS OF THE EXPERIMENTAL RUN**

| | |
|---|---|
| Study interval | 13 h |
| Rainfall rate | 10.8 $\mu$m/s |
| Base-level fall rate | 3.1 $\mu$m/s |
| Average time step between photographs | 7 min |
| Number of photographs evaluated | 96 |
| Number of hill slope failures mapped | 505 |
| Smallest failure detected | 1.4 $cm^2$ |
| Largest failure detected | 62.8 $cm^2$ |
| Mean failure area | 11.1 $cm^2$ |
| Basin area | 6400 $cm^2$ |

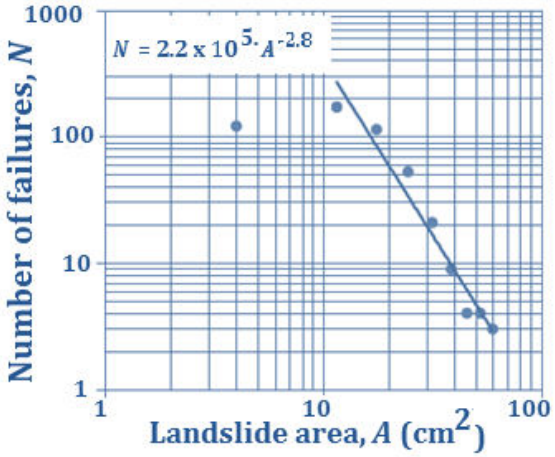


Figure 9. Frequency distribution of hillslope failures during a 13 h period under steady erosion conditions. Typical of landslide distributions in natural settings, the distribution exhibits power-law scaling, though the range in failure size is smaller than for natural settings. The power law on the diagram yields the number of failures ($N$) of a given area ($A$). Decreasing numbers of small events could result from difficulty in detection, or represent a lower limit to mass movement size.

Knickpoint locations were also measured from the same set of photographs. Three major knickpoint events initiated within 20 cm of the outlet and propagated throughout the basin. Nine other knickpoints initiated 20-50 cm from the outlet. Of these, some propagated to the edges of the basin, while others dissipated. Such behavior has been observed in other studies (Parker, 1977; Hancock, 1997). Migration speed for knickpoints in trunk streams was ~0.6 cm/min; in the upper part of the experimental basin, Decreased velocities (~0.4 cm/min) were measured as the knickpoint migrated into smaller tributaries.

**Spatial Patterns and Relationships Between Hillslope Failures, Knickpoints, and Temporary Sediment Storage**

The main purpose of this study was to identify and characterize the possible presence of patterns in the spatial distribution of landslides, and determine what, if any, relationship exists between landslides and knickpoints. Before it is searched for relationships between processes, it is helpful to know if any pattern is detectable in the spatial distribution of hillslope failures. Hence, a null hypothesis might be that hillslope failures are randomly distributed in space across the landscape. To test this hypothesis, it was applied that a Monte Carlo simulation technique (Metropolis, 1987). It was numerically generated 100 sets of 505 randomly located landslides over the experimental basin, so that observed and synthetic hillslope failures were equal in number. It was then analyzed the clustering tendency in experimental and random distributions of landslides. A qualitative visual inspection of failure locations for a 4 h period mapped onto a single image (Fig. 10) suggests that some clustering exists in the experimental data.

Clustering tendency was determined by measuring for each failure, $i$, the distance $w_i$. to the closest landslide $j$, for both randomly distributed and experimental data sets. It was indicated that the distance between the centroids of landslide $i$ and $j$ with $d_{ij}; w_i$ is computed accordingly to the relationship

$$w_i = \begin{matrix} N \\ \min d_{i,j} \\ j = 1 \\ j \neq i \end{matrix} \quad (1)$$

for $i$ = 1,..., $N$, where $N$ = 505 is the number of observed landslides in the considered time interval. The sample frequency distribution of $w_i$, computed for the experimental data is shown in Figure 11, along with the 90% confidence envelope of the frequency distribution of $w_i$, computed on the 100 random sets of 505 landslides. It cannot be rejected that the hypothesis that the minimum distance among landslides is slightly lower in the experimental basin at the 90% confidence level. Even at a

98% confidence limit, some clustering is still apparent in the experimental data. This latter outcome confirms that both spatial ordering as well as randomness contribute to the stochastic nature of slope failures in the experimental landform.

The analysis above does not take into account the relation of failures to knickpoint locations. It is known that knickpoints account for a significant amount of incision in the basin, and hence they should contribute to destabilization of hillslopes. Their effects were quantified by focusing on failures along a single channel and counting the number of landslides that occurred upstream and downstream from knickpoint locations. This resulted in 47 failures downstream and 13 failures upstream from knickpoint locations. Clearly, the greater number of landslides downstream could be evidence of knickpoint triggering. However, this could also result from knickpoint location. For instance, a concentration of knickpoints in the upper part of the trunk stream could result in a high number of downstream hillslope failures even if landslides were randomly distributed. An initial test was performed on the size of failures upstream and downstream from a knick point to test for any bias in the actual volume of material removed by failures. Are failures downstream from knick points larger than upstream? In order to check from a statistical point of view whether or not significant differences exist, the probability density functions of upstream and downstream landslides were estimated. Figure 12 shows the obtained sample probability density functions. A quantitative comparison was carried out between the mean values and the standard deviations of the two distributions. The 90% confidence limits of the estimated mean values of upstream and downstream hillslope failure areas are 11.81-20.91 $cm^2$ and 13.98-19.24 $cm^2$, respectively. The 90% confidence limits of the estimated standard deviations of upstream and downstream hillslope failure areas are 7.56-15.16 $cm^2$ and 9.42-13.32 $cm^2$, respectively. Since mean and standard deviations between the two populations overlap substantially, one cannot reject (at the 90% confidence level) the hypothesis that mean and standard deviation of upstream and downstream landslide areas are identical. The similarity of the two probability density functions is also clearly shown in Figure 12. This analysis allows us to conclude that no significant link exists between landslide size and knickpoint location. It was then turned to analyzing the significance of increased numbers of landslides downstream from knickpoints by means of another Monte Carlo simulation. Since landslide area statistics are invariant upstream and downstream from knickpoints, the number of landslides is directly related to total landslide area. 100 random data sets of an equal number ($N = 60$) was generated of hillslope failures along the trunk stream and computed the mean and 90% confidence bands for downstream events. The results are reported in Table 2. The mean number of downstream landslides in the Monte Carlo experiments is 40, with a 90% upper confidence limit of 44. This is slightly lower than the experimental result ($n = 47$). Therefore, one cannot reject the hypothesis, at the 90% confidence level, that downstream landslides occur less frequently in the random scenario than in the experimental basin. Indeed, the above hypothesis cannot be rejected for a confidence level up to 98%.

Efforts were made by considering the along-stream distance $x_t$ between a knickpoint at time $t$ (the time each photograph was taken) and the experimental landslides at the same time $t$ that occurred downstream on the trunk stream. Then it was repeated that the Monte Carlo analysis by developing 100 sets of 47 downstream randomly located events, while maintaining the same knickpoint positions as observed in the experimental run. This allowed us to get 100 sets of 47 random distances, which is designated with the symbol $x^*_t$.

A comparison between the experimental probability density functions of $x_t$ and the 90% confidence envelope of the Monte Carlo-generated probability density functions of $x^*_t$ is shown in Figure 13. Clearly, the probability density function of experimental landslides is significantly different in this scenario from that obtained with a random distribution. In the Monte Carlo simulations, the probability density function is unimodal. The mode of the distribution, $x^*_m$, indicates the most probable distance between knickpoints and downstream landslides if the locations were random. The magnitude of $x^*_t$ is determined by the geometry of the system and the statistical behaviors of the above stochastic processes. For instance, a knickpoint moving with lower velocity in the upper part of the basin would lead to a smaller value of $x^*_m$.

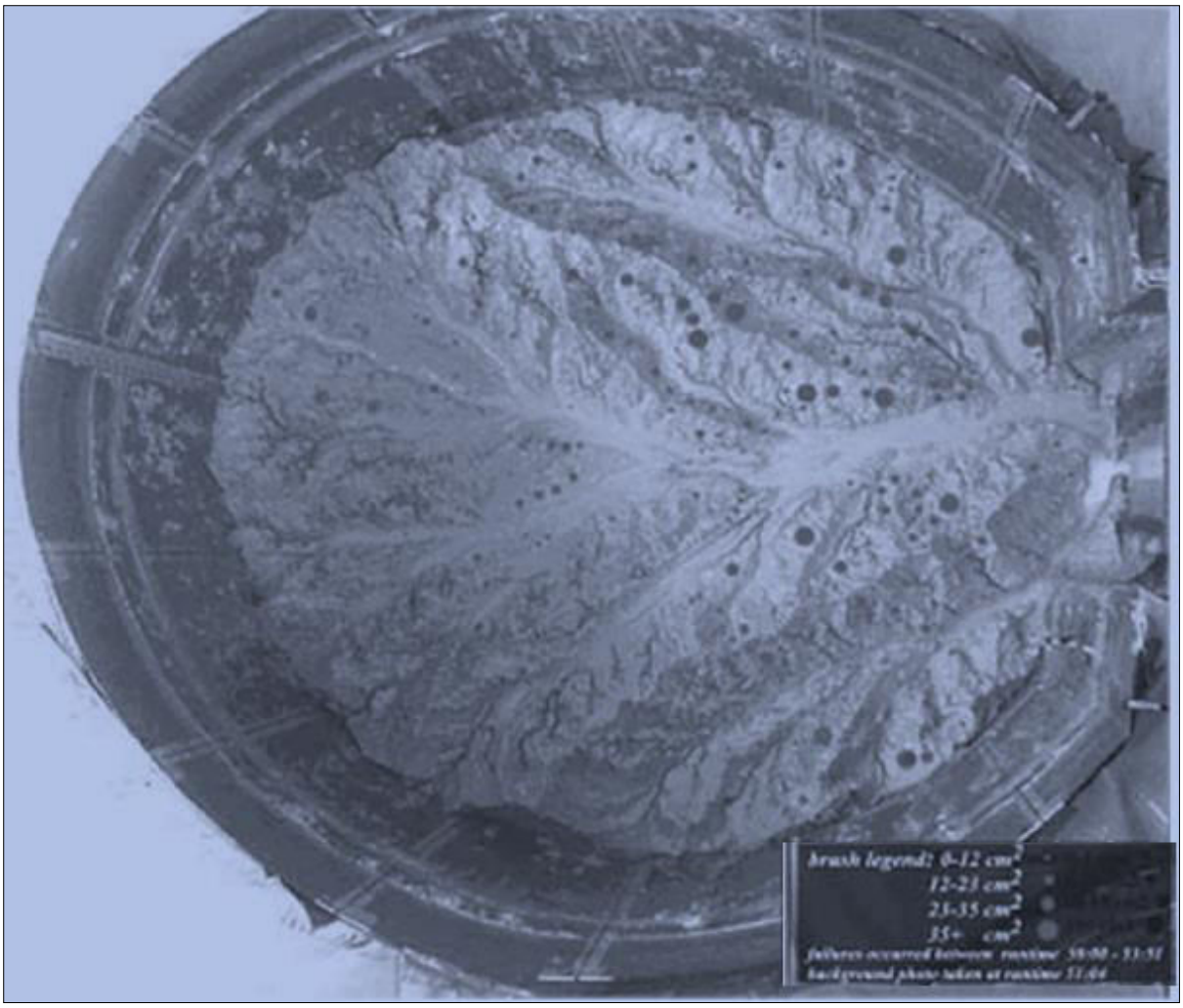


Figure 10. Hill slope failures that occurred during a 4 h period (from 50:08 h to 53:51 h), plotted as gray circles onto a photograph taken at the beginning of the 4 h period, with area proportional to actual failure area. Some clustering of failures is apparent in the photograph; see text for analysis of the significance of this clustering.

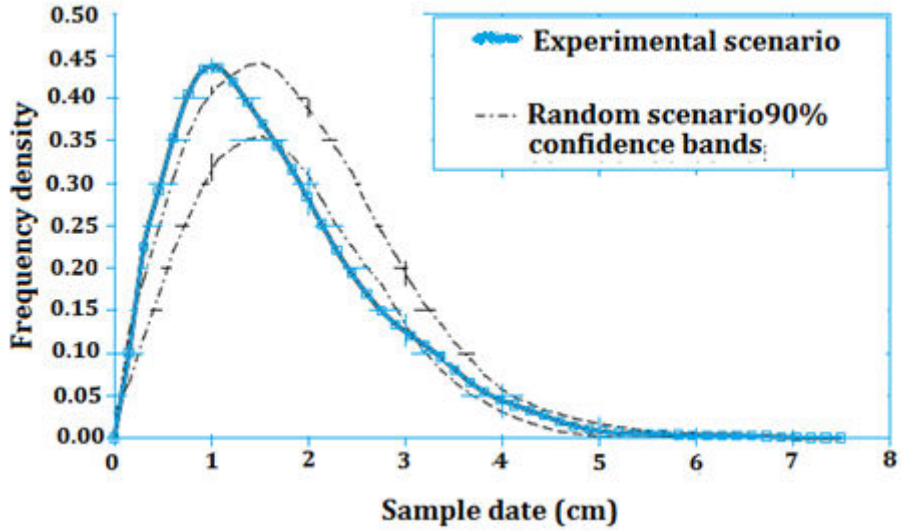


Figure 11. Comparison between the sample frequency distributions of the minimum distance between landslides for experimental and Monte Carlo simulated landslides. Random and experimental distributions are similar. However, the peak frequency at 1 cm separation distance suggests tighter clustering for experimental landslides.

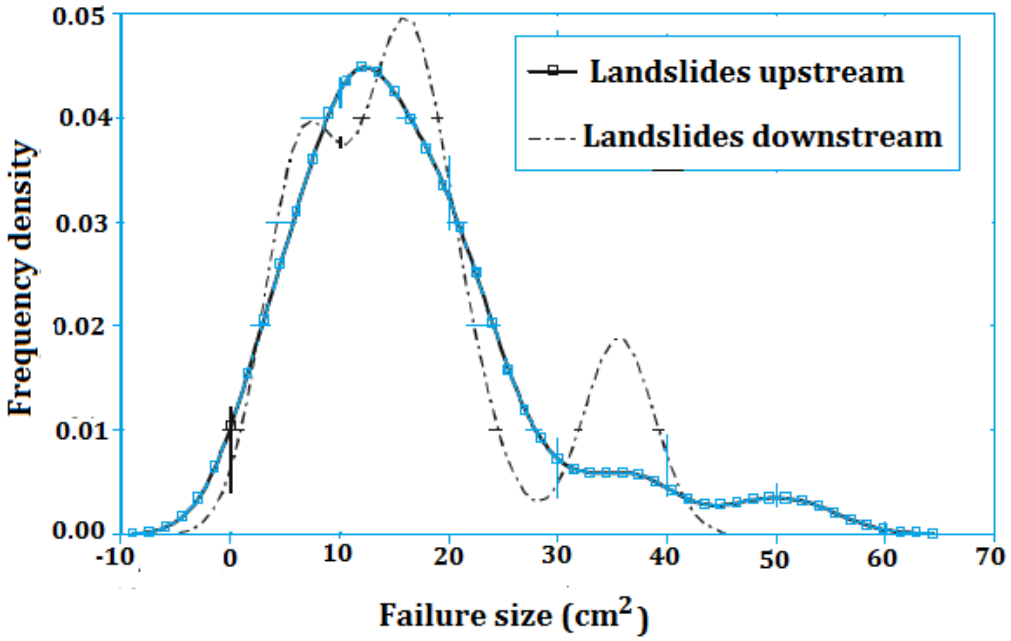


Figure 12. Comparison between the sample frequency distributions of the landslide area (that is, size) that occurred in the main channel upstream and downstream of knickpoints.

TABLE 2. NUMBER OF LANDSLIDES LOCATED DOWNSTREAM AND UPSTREAM OF KNICKPOINTS IN THE RANDOM AND EXPERIMENTAL LANDSLIDE DISPLACEMENT MODELS

| Landslide displacement | Number of landslides downstream from a knickpoint | Number of landslides upstream from a knickpoint |
|---|---|---|
| Random (100 simulations) | 40 (36–44) | 20 (24–16) |
| Experimental | 47 | 13 |

*Note*: For the random location, the mean values computed in 100 simulations are given, along with the respective 90% confidence limits (shown in parentheses).

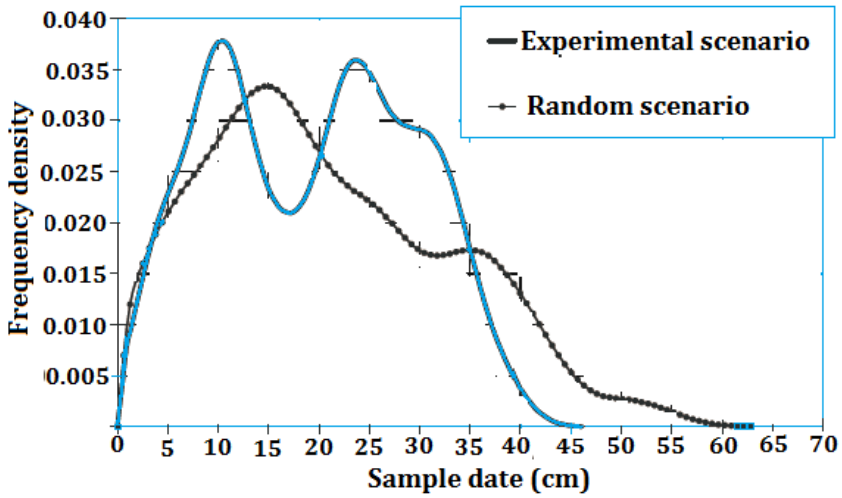


Figure 13. Comparison between the sample frequency distributions of the distances between landslides and closest upstream knickpoint in the experiment and in the random displacements. Experimental frequency distribution is bimodal, with peaks at 10 and 24 cm. A random distribution exhibits a single peak at 10 cm.

The experimental data are characterized by a bimodal probability density function. The value of the first mode, $x_1$, is close to the value of $x^*_m$, which is suggestive of significant landslide triggering unrelated to knickpoints. However, the presence of a second mode, $x_2$, suggests the possible presence of a landslide triggering effect induced by knickpoint migration. The parameter $x_2$ is a characteristic distance between knickpoints and downstream hillslope failures induced by them. The value of $x_2$ is ~24 cm and represents a delay distance between the passage of a knickpoint and landslide activation. The hypothesis of the presence of statistically significant differences between the probability density functions of observed and simulated $x^*_t$ cannot be rejected for a confidence level up to 99%.

One final analysis was performed on the relationship between failures and knickpoint locations. For the *i*th landslide in the main channel that collapsed during the last 13 h of the experiment downstream from a knickpoint, for $i$ ranging from 1 to 47, the distance $h_i$. from the basin outlet was recorded, as well as the distance $k_i$ from the basin outlet to the closest upstream knick-point. Therefore, 47 couples $(h_i, k_i)$ were collected. If a relationship exists between $h_i$ and $k_i$ one would expect to see a significant cross-correlation between them. Indeed, the cross-correlation coefficient between the couples $(h_i, k_i)$ is 0.65. A Monte Carlo simulation was performed as a null hypothesis by computing the cross-correlation coefficient between the vector of the $k$ values and 1000 vectors obtained by randomly generating the $h_i$ distances, from a uniform distribution, in the range $[0, k_i]$, thereby breaking the connection between the locations of landslides and the corresponding knickpoint closest upstream. A sample of 1000 values of cross-correlation was generated coefficients between knickpoint positions and randomly distributed downstream landslides. The mean value of the sample is equal to 0.45 and the upper 90% confidence limit is 0.59. The observed value of the cross-correlation coefficient was exceeded in 6 out of 1000 synthetic random realizations. Therefore, one cannot reject the hypothesis of the presence of a significant relationship between knickpoints and downstream landslides positions at the 99% confidence level. This analysis confirms the findings obtained with the previous investigations.

**Discussion**

Experiments were conducted under steady rainfall and base-level fall conditions. This effectively removed landslide triggering events, such as severe storms and earthquakes, from consideration, and allowed us to focus on stream incision as the dominant triggering mechanism. In a landscape where streams incise continuously at a constant rate, one might expect that hill-slope failures would occur as local conditions for instability are met, and a spatial pattern of landslides independent of knickpoint position would result. If stream incision varies in a systematic way, such as that which occurs during upstream migration of a knickpoint, failure patterns should exhibit clustering downstream from the knickpoint. Interestingly, a synoptic basin-scale view of failures in the experiment revealed a statistically significant tendency to clustering at the 98% confidence level. In particular, by selecting failures along a stream and correlating failure locations with knickpoint locations, a statistically significant link was observed. In particular, it was found that hillslope failures are more likely to occur downstream from a knickpoint.

In fact, the results of the three quantitative analyses carried out to test the hypothesis that stream incision by migrating knickpoints can impose a spatial and temporal pattern on landslide distributions are consistent. They show that one cannot reject the above hypothesis with a confidence level ranging from 98% and 99%. Therefore, a high probability exists that a significant relation between knickpoint and landslide positions is indeed present, even if this result must be interpreted in a statistical sense, i.e., the relation is likely to be present but not certain. The significance of this conclusion, which comes from three different analyses that ended up with consistent results, can be evaluated in view of its confidence level, which is an indication of how strong the relation is. Of course, the spatial pattern of landslides is also affected by the presence of significant hillslope triggering factors that are not related to knickpoint migration.

The following exercise was offered to get some sense of the knickpoint contribution to overall stream incision. Recall that experiment was conducted at steady base-level fall under flux steady-state conditions. This implies that, on average, stream incision is equal to the base-level fall rate, in this case 3.1 um/s. Under these conditions, it can be estimated that the contribution of knickpoints to overall stream incision. 12 knickpoint events were observed during the time it was measured at knick-

point and hillslope failure locations. During this observational time (13 h), base level dropped 14.5 cm. While knickpoint heights varied, and most knickpoints initiated at a location upstream from the outlet, nonetheless limits can set on knickpoint contribution by assuming that the average knick-point height was 0.5 cm, and that this height was maintained while the knickpoint propagated through the entire stream network. Given these assumptions, knickpoints account for 6 cm of incision, or nearly half of the total stream incision during the observation period. If stream incision by knickpoints is the only destabilizing factor, then this implies that knickpoints are responsible for ~50% of the failures. When this estimate is compared to the number of failures downstream ($n$ = 47) from a knickpoint to the total failures along the stream ($n$ = 60), it was found in a higher percentage (78%). Note that this calculation likely includes some failures that result from steady stream incision downstream from the knickpoint. The point made here is that streams incise in the experiment via both knickpoint propagation and steady bed lowering. Given these two mechanisms of incision, it is not surprising that the relationship between knickpoint and failure locations is statistically significant. It can also be concluded that knickpoint incision plays a significant role in destabilizing hillslopes.

Large mean separation distance (24 cm) observed between knickpoints and landslides triggered by them are somewhat astonishing. This could explain the time required for base-level lowering in the channel to propagate laterally to the toe of the hillslope (recall that channels typically narrow and deepen around a knickpoint). Hillslopes adjacent to channels in v-shaped valleys that lack a floodplain would respond more rapidly to stream incision than hillslopes bordering wide valleys. So far as landslide area is concerned, no significant difference was found depending on knickpoint position. As a matter of fact, the probability density functions of hill-slope failure size were not significantly different for events downstream and upstream from knickpoints. This result seems to indicate that the landslide size in the experiment was not significantly different for events triggered by knickpoint migration than by other causes.

Do natural eroding drainage basins behave like the model? This, of course, no answer can be given definitively. This experiment was not a scaled model of a natural prototype. In fact, it is not possible to construct a scale model with the linear dimensions of the tank that captures the flow conditions of a larger drainage basin. The experimental streams are dominated by laminar flow (maximum Reynolds number is ~750), whereas natural mountain streams are always turbulent. It is observed that significant overlap in Froude numbers between experimental and natural drainages (both are dominantly subcritical, with some stream sections at or above critical flow). Sediment concentration for the experiment presented here approached 25%, and such concentrations are unusual in natural rivers (though not unheard of). Feedback between local deposition and erosion may be enhanced at this concentration and could be a source of instability within model streams (Hasbargen and Paola, 2000). Flow depth to grain size ratios vary downstream in the experiment, but for flow depths on the order of 1 mm, this ratio was ~20. Natural streams typically have much higher ratios. A gravel-bedded stream with 1 cm grains and 1 m depth, for instance, has a depth to grain size ratio of 100. The target was not to build two replica of a natural landscape, but to represent the major processes in a setting in which could be isolated and analyze landscape interactions that would take an extremely long time in nature. It is not felt that any of the scale effects noted above would cause qualitatively different dynamics between knickpoints and landslides. The existence of additional features and processes in a landscape, such as vegetation, gophers, tree throw, creep, weathering and soil development, storm and earthquake events, road construction, etc., would add greater complexity to natural systems. It is expected that such effects are to complicate and obscure stochastic interactions between streams and hillslopes. While there are significant differences between the model landscape and natural settings, the approximate similarity of landscape features and of process activity (failure sizes on the order of the hillslope length; hillslopes of ~90% slope; knickpoint heights on the order of several flow depths) suggests that natural landscapes experiencing stream incision and knickpoint propagation might also exhibit similar dynamics. Indeed, large number of failures downstream from knickpoint has been noted in natural settings. This result reflects on the role of stream incision in destabilizing hillslopes. In the absence of external stochastic triggers, such as storm events and earthquakes, it is still found that hillslope failures are strongly stochastic. Part of the variability can be ascribed to local conditions, such as slope steepness, pore fluid pressure, past history of failures, etc. Part of the control on landslides, however, is exerted by conditions at the toe of the hillslope. Stream

incision, either via steady downcutting or by episodic knickpoint propagation, can introduce a weak structure to spatial patterns of landslides.

This observation suggests that spatial patterns of hillslope failures could be a result of recent incision by streams at the toe of the hillslopes. This study, which must now be checked against natural settings, could allow for fast identification of regions in a drainage basin prone to increased landscape instability. So far as it is concerned with landslide forecasting in mountainous landscapes, locations downstream from knickpoints merit special attention.

## Conclusion

The results were presented from a small-scale erosion experiment under constant forcing conditions where it focused attention on the relationship between hillslope failure activity and knickpoint migration. Measurement of landslide sizes and locations and knickpoint locations were taken over time under steady forcing conditions. The possible existence of spatial organization of hillslope failures was tested, such as clustering, using randomly generated spatial distributions of landslides as a reference. A statistically significant relation was observed between knickpoint positions and downstream landslide location. The detection of a significant link between migrating knickpoints and landslides confirms the intuition concerning the effectiveness of knickpoints in triggering failures. It is noted, however, that stream downcutting in the absence of knickpoint propagation, and local effects like slope and pore pressure, also control hillslope stability. These effects superimpose a random spatial component onto the spatial patterns associated with knickpoint migration.

## References


Ahnert, F., 1998, Introduction to geomorphology: London, Arnold, 360 p.

Alonso, C.V., Bennett, S.J., and Stein, O.R., 2002, Predicting headcut erosion and migration in concentrated flows typical of upland areas: Water Resources Research, v. 38, p. 39-1-39-15.

Benda, L., and Dunne, T., 1997, Stochastic forcing of sediment supply to channel networks from landsliding and debris flow: Water Resources Research, v. 33, p. 2849-2863, doi: 10.1029/97WR02388.

Bennett, S.J., Alonso, C.V., Prasad, S.N., and Roemkens, M.J.M., 2000, Experiments on headcut growth and migration in concentrated flows typical of upland areas: Water Resources Research, v. 36, p. 1911-1922, doi:

Brardinoni, F., and Church, M., 2004, Representing the landslide magnitude-frequency relation: Capilano River basin, British Columbia: Earth Surface Processes and Landforms, v. 29, p. 115-124, doi: 10.1002/esp.1029.

Brush, L.M., Jr., and Wolman, G., 1960, Knickpoint behavior in noncohesive material—A laboratory study: Geological Society of America Bulletin,v. 71, p. 59-73.

Bryan, R.B., 1990, Knickpoint evolution in rillwash, *in* Bryan, R.B., ed., Soil erosion—Experiments and models: Catena Supplement, v. 17, p. 111-132.

Bryan, R.B., and Rockwell, D.L., 1998, Water table control on rill initiation and implications for erosional response: Geomorphology, v. 23, p. 151-169, doi: 10.1016/S0169-555X(97)00110-4.

Burbank, D.W., Leland, J., Felding, E., Anderson, R.S., Brozovic, N., Reid, M.R., and Duncan, C., 1996, Bedrock incision, rock uplift and threshold hillslopes in the northwestern Himalayas: Nature, v. 379, p. 505-510, doi: 10.1038/379505a0.

Burton, A., Arkell, T.J., and Bathurst, J.C., 1998, Field variability of landslide model parameters: Environmental Geology, v. 35, p. 100-114, doi: 10.1007/s002540050297.

Campbell, R.H., 1975, Soil slips, debris flows and rainstorms in the Santa Monica Mountains and vicinity, Southern California: U.S. Geological Survey Professional Paper 851, 51 p.

Cantelli, A., Paola, C., and Parker, G., 2004, Experiments on upstream-migrating erosional narrowing and widening of an incisional channel caused by dam removal: Water Resources Research, v. 40, p. W03304, doi: 10.1029/2003WR002940.

Casadei, M., Dietrich, W.E., and Miller, N.L., 2003, Testing a model for predicting the timing and location of shallow landslide initiation in soil-mantled landscapes: Earth Surface Processes and Landforms, v. 28, p. 925-950, doi: 10.1002/esp.470.

Crosby, B.T., and Whipple, K.X., 2002, Knickpoint migration in the Waipaoa River: An examination of the rate and form of transient behavior in fluvial networks: Eos (Transactions, American Geophysical Union), v. 83(47), Fall meeting supplement, abstract H21G-10.

Crozier, M.J., Deimel, M.S., and Simon, J.S., 1995, Investigation of earthquake triggering for deep-seated landslides, Taranaki, New Zealand: Quaternary International, v. 25, p. 65-73, doi: 10.1016/1040-6182(94)00036-5.

Dadson, S.J., Hovius, N., Chen, Hongey, Dade, W.B., Hsieh, Meng-Long, Willett, S.D., Hu, Jyr-Ching, Horng, Ming-Jame, Chen, Meng-Chiang, Stark, C.P., Lague, D., and Lin, Jiun-Chuan, 2003, Links between erosion, runoff variability and seismicity in the Taiwan orogen: Nature, v. 426,p. 648-651.

Densmore, A.L., and Hovius, N., 2000, Topographicfingerprints of bed-rock landslides: Geology, v. 28, p.371-374, doi: 10.1130/0091-7613(2000)028<371:TFOBL>2.3.CO;2.

Densmore, A.L., Anderson, R.S., McAdoo, B.G., and Ellis, M.A., 1997, Hill-slope evolution by bedrock landslides: Science,

v. 275, p. 369-372, doi:\10.1126/science.275.5298.369.
Dietrich, W.E., and Dunne, T., 1993, The channel head, *in* Beven, K., and Kirkby, M.J., eds., Channel network hydrology: New York, John Wiley,p. 175-219.
Dietrich, W.E., Reiss, R., Hsu, M., and Montgomery, D.R., 1995, A process-based model for colluvial soil depth and shallow landsliding using digital elevation data: Hydrological Processes, v. 9, p. 383-400.
Duan, J., 1996, A coupled hydrologic-geomorphic model for evaluating effects of vegetation change on watersheds, [Ph.D. thesis]: Corvallis, Oregon, Oregon State University, 133 p.
Gabet, E.M., and Dunne, T., 2002, Landslides on coastal sage-scrub and grassland hillslopes in a severe El Nino winter: The effects of vegetation conversion on sediment delivery: Geological Society of America Bulletin, v. 114, p. 983-990, doi: 10.1130/0016-7606(2002)114<0983:LOCSSA>2.0.CO;2.
Gardner, T.W., 1983, Experimental study of knickpoint and longitudinal profile evolution in cohesive, homogeneous material: Geological Society of America Bulletin, v. 94, p. 644-672, doi: 10.1130/0016-7606(1983)94<664:ESOKAL>2.0.CO;2
Guzzetti, F., Malamud, B.D., Turcotte, D.L., and Reichenbach, P., 2002, Power-law correlations of landslide areas in central Italy: Earth and Planetary Science Letters, v. 195, p. 169-183, doi: 10.1016/S0012-821X(01)00589-1.
Hancock, G., 1997, Experimental testing of the Siberia landscape evolution model [Ph.D. thesis]: Newcastle, New South Wales, Australia, University of Newcastle, 467 p.
Hancock, G.S., Anderson, R.S., and Whipple, K.X., 2003, Beyond power: Bedrock river incision process and form, *in* Tinkler, K., and Wohl, E., eds., Rivers over rock: Fluvial processes in bedrock channels: American Geophysical Union Geophysical Monograph 107, p. 35-60.
Harp, E.L., and Jibson, R.L., 1995, Inventory of landslides triggered by the 1994 Northridge, California, earthquake: U.S. Geological Survey Open-File Report 95-213, 18 p.
Hasbargen, L.E., and Paola, C., 2003, How predictable is local erosion rate in erosional landscapes?, *in* Wilcox, P.R., and Iverson, R.M., eds., Prediction in geomorphology: American Geophysical Union Geophysical Monograph 135, 256 p.
Hasbargen, L.E., 2003, Erosion in steady state drainage basins [Ph.D. thesis]: Minneapolis, Minnesota, University of Minnesota, 228 p.
Hasbargen, L.E., and Paola, C., 2000, Landscape instability in an experimental drainage basin: Geology, v. 28, p. 1067-1070, doi: 10.1130/0091-7613(2000)028<1067:LIIAED>2.3.CO;2.
Havenith, H.B., Strom, A., Jongmans, D., Abdrakhmatov, K., Delvaux, D., and Trefois, P., 2003, Seismic triggering of landslides, Part A: Field evidence from the northern Tien Shan: Natural Hazards and Earth System Science, v. 3, p. 135-149.
Hermanns, R.L., Trauth, M.H., Niedermann, S., McWilliams, M., and Strecker, M.R., 2000, Tephrochronologic constraints on temporal distribution of large landslides in northwest Argentina: Journal of Geology, v. 108, p. 35-52, doi: 10. 1086 /314383.
Holland, W.N., and Pickup, G., 1976, Flume study of knickpoint development in stratified sediment: Geological Society of America Bulletin, v. 87, p. 76-82, doi: 10.1130/0016-7606(1976)87 <76:FSOKDI> 2.0.CO;2.
Hovius, N., Stark, C.P., and Allen, P.A., 1997, Sediment flux from a mountain belt derived by landslide mapping: Geology, v. 25, p. 231-234, doi: 10.1130/0091-7613(1997)025<0231:SFFAMB>2.3.CO;2.
Iida, T., 1984, A hydrological method of estimation of the topographic effect on the saturated through flow: Transactions, Japanese Geomorphologic Union, v. 5, p. 1-12.
Iverson, R.M., 2000, Landslide triggering by rain infiltration: Water Resources Research, v. 36, p. 1897-1910, doi: 10.1029 /2000WR900090.
Keefer, D., 1994, The importance of earthquake-induced landslides to long-term slope erosion and slope-failure hazards in seismically active regions: Geo-morphology, v. 10, p. 265-284, doi: 10.1016/0169-555X(94)90021-3.
Lague, D., Crave, A., and Davy, P, 2003, Laboratory experiments simulating the geomorphic response to tectonic uplift: Journal of Geophysical Research, v. 108(B1), ETG 3-1-3-20.
Larsen, M.C., and Parks, J.E., 1997, How wide is a road? The association of roads and mass-wasting in a forested montane environment: Earth Surface Processes and Landforms, v. 22, p. 835-848, doi: 10.1002/(SICI)1096-9837 (199709) 22:93.3.CO;2-3.
Larsen, M.C., and Torres-Sanchez, A.J., 1998, The frequency and distribution of recent landslides in three montane tropical regions of Puerto
Rico: Geomorphology, v. 24, no. 4, p. 309-331, doi: 10.1016/S0169-555X(98)00023-3.
Martin, Y., Rood, K., Schwab, J.W., and Church, M., 2002, Sediment transfer by shallow landsliding in the Queen Charlotte Islands, British Columbia: Canadian Journal of Earth Sciences, v. 39, p. 189-205, doi: 10.1139/e01-068.
Merritt, E., 1984, The identification of four stages during micro-rill development: Earth Surface Processes and Landforms, v. 9, p. 493-496.
Metropolis, N., 1987, The beginning of the Monte Carlo method: Los Alamos Science, v. 15, p. 125-130.
Miller, D.J., and Sias, J., 1998, Deciphering large landslides: Linking hydrological, groundwater and slope stability models through GIS: Hydrological Processes, v. 12, p. 923-941, doi: 10.1002/(SICI)1099-1085 (199805)12:63.0.CO;2-3.
Miller, J.R., 1991, The influence of bedrock geology on knickpoint development and channel-bed degradation along downcutting streams in south-central Indiana: Journal of Geology, v. 99, p. 591-605.
Montgomery, D.R., and Dietrich, W.E., 1994, A physically-based model for the topographic control on shallow landsliding: Water Resources Research, v. 30, p. 1153-1171, doi: 10.1029/93WR02979.
Montgomery, D.R., Schmidt, K.M., Greenberg, H.M., and Dietrich, W.E., 2000,Forest clearing and regional landsliding: Geology, v. 28, p. 311-314, doi:10.1130/0091-7613(2000)028<311:FCARL>2.3.CO;2.
Mosley, M.P., 1974, Experimental study of rill erosion: Transactions of American Society of Agricultural Engineering, v.

17, p. 909-913.
Parker, G., and Izumi, N., 2000, Purely erosional cyclic and solitary steps created by flow over cohesive bed: Journal of Fluid Mechanics, v. 419,p. 203-238, doi: 10.1017/S0022112000001403.
Parker, R.S., 1977, Experimental study of basin evolution and its hydrologic implications [Ph.D. thesis]: Fort Collins, Colorado, Colorado State University, 331 p.
Peakall, J., Ashworth, P.J., and Best, J.L., 1996, Physical modelling in fluvial geomorphology; principles, applications and unresolved issues, *in* Rhoads, B.L., and Thorn, C.E., eds., The scientific nature of geomorphol-ogy: Chichester, Wiley, p. 221-253.
Roering, J.J., Kirchner, J.W., Sklar, L.S., and Dietrich, W.E., 2001, Hillslope evolution by nonlinear creep and landsliding: An experimental study: Geology, v. 29, p. 143-146, doi: 10.1130/0091
Schumm, S.A., 1956, Evolution of drainage systems and slopes in badlands at Perth Amboy, New Jersey: Geological Society of America Bulletin, v. 67,p. 597-646.
Schuster, R.L., and Highland, L.M., 2001, Socioeconomic and environmental impacts of landslides in the Western Hemisphere : U.S. Geological SurveyOpen-File Report 01-0276.
Selby, M.J., 1982, Hillslope materials and processes: Oxford, Oxford University Press, 466 p.
Sidle, R.C., 1992, A theoretical model of the effects of timber harvesting on slope stability: Water Resources Research, v. 28, p. 1897-1910, doi:10.1029/92WR00804.
Sklar, L., and Dietrich, W.E., 2003, River longitudinal profiles and bedrock incision models: Stream power and the influence of sediment supply, *in* Tinkler, K., and Wohl, E., eds., Rivers over rock: Fluvial processes in bedrock channels: American Geophysical Union Geophysical Monograph107, p. 237-260.
Slattery, M.C., and Bryan, R.B., 1992, Hydraulic conditions for rill incision under simulated rainfall: A laboratory Experiment : Earth Surface Processes and Landforms, v. 17, p. 127-146.
Stark, C.P., and Hovius, N., 2001, The characterization of landslide size distributions: Geophysical Research Letters, v. 28, p. 1091-1094, doi: 10.1029/2000GL008527.
Stock, J., and Dietrich, W.E., 2003, Valley incision by debris flows: Evidence of a topographic signature: Water Resources Research, v. 39, p. ESG 11-1-25.
Terzaghi, K., Peck, R.B., and Mesri, G., 1996, Soil mechanics in engineering practice: New York, Wiley, 549 p.
Trauth, M.H., Alonso, R.A., Haselton, K.R., Hermanns, R.L., and Strecker, M.R., 2000, Climate change and mass movements in the NW Argentine Andes: Earth and Planetary Science Letters, v. 179, p. 243-256, doi: 10.1016/S0012-821X(00)00127-8.
van Asch, T.W.J., and van Steijn, H., 1991, Temporal patterns of mass movements in the French Alps: Catena, v. 18, p. 515-527, doi: 10.1016/0341-8162(91)90052-Y.
Willett, S.D., and Brandon, M.T., 2002, On steady state mountain belts: Geology, v. 30, p. 175-178, doi: 10.1130/0091-\ 7613(2002)030<0175: OSSIMB>2.0.CO;2.
Wohl, E., 2003, Bedrock channel morphology in relation to erosional processes, *in* Tinkler, K., and Wohl, E., eds., Rivers over rock: Fluvial processes in bedrock channels: American Geophysical Union Geophysical Monograph 107, p. 133-151.
Zaprowski, B.J., Evenson, E.B., Pazzaglia, F.J., and Epstein, J.B., 2001, Knickzone propagation in the Black Hills: A different perspective on the late Cenozoic exhumation of the Laramide Rocky Mountains:Geology, v. 29, p. 547-550, doi: 10.1130/0091-7613(2001)029<0547: KPITBH>2.0.CO;2.MANUSCRIPT ACCEPTED BY THE SOCIETY 23 JUNE 2005